

1 **High-Resolution Meteorological Forcing Data for Hydrological Modelling and Climate Change**  
2 **Impact Analysis in Mackenzie River Basin**

3  
4 **Zilefac Elvis Asong<sup>1</sup>, Mohamed Ezzat Elshamy<sup>1</sup>, Daniel Princz<sup>1</sup>, Howard Simon Wheeler<sup>1</sup>, John W.**  
5 **Pomeroy<sup>1,2</sup>, Alain Pietroniro<sup>1,2,3</sup> and Alex Cannon<sup>4</sup>**

6  
7 *<sup>1</sup>Global Institute for Water Security, University of Saskatchewan, 11 Innovation Blvd, Saskatoon, SK,*  
8 *Canada S7N 3H5*

9  
10 *<sup>2</sup>Centre for Hydrology, University of Saskatchewan, 121 Research Drive, Saskatoon, SK, Canada S7N 1K2*

11  
12 *<sup>3</sup>Environment and Climate Change Canada, 11 Innovation Blvd, Saskatoon, SK, Canada S7N 3H5*

13  
14 *<sup>4</sup>Climate Research Division, Environment and Climate Change Canada, BC V8W 2Y2, Victoria, Canada*

15  
16 **\*Corresponding author:**

17 Phone: +1 306 491 9565

18 Email: [elvis.asonq@usask.ca](mailto:elvis.asonq@usask.ca)

28 **Abstract**

29 Cold regions hydrology is very sensitive to the impacts of climate warming. Impacts of warming over  
30 recent decades in western Canada include glacier retreat, permafrost thaw and changing patterns of  
31 precipitation, with an increased proportion of winter precipitation falling as rainfall and shorter durations  
32 of snowcover, and consequent changes in flow regimes. Future warming is expected to continue along  
33 these lines. Physically realistic and sophisticated hydrological models driven by reliable climate forcing can  
34 provide the capability to assess hydrological responses to climate change. However, the provision of  
35 reliable forcing data remains problematic, particularly in data sparse regions. Hydrological processes in  
36 cold regions involve complex phase changes and so are very sensitive to small biases in the driving  
37 meteorology, particularly in temperature and precipitation, including precipitation phase. Cold regions  
38 often have sparse surface observations, particularly at high elevations that generate a large amount of  
39 runoff. This paper aims to provide an improved set of forcing data for large scale hydrological models for  
40 climate change impact assessment. The best available gridded data in Canada is from the high-resolution  
41 forecasts of the Global Environmental Multiscale (GEM) atmospheric model and outputs of the Canadian  
42 Precipitation Analysis (CaPA) but these datasets have a short historical record. The EU WATCH ERA-Interim  
43 reanalysis (WFDEI) has a longer historical record but has often been found to be biased relative to  
44 observations over Canada. The aim of this study, therefore, is to blend the strengths of both datasets  
45 (GEM-CaPA and WFDEI) to produce a less-biased long record product (WFDEI-GEM-CaPA) for hydrological  
46 modelling and climate change impacts assessment over the Mackenzie River Basin. First, a multivariate  
47 generalization of the quantile mapping technique was implemented to bias-correct WFDEI against GEM-  
48 CaPA at  $3h \times 0.125^\circ$  resolution during the 2005-2016 overlap period, followed by a hindcast of WFDEI-  
49 GEM-CaPA from 1979. The derived WFDEI-GEM-CaPA data are validated against station observations as a  
50 preliminary step to assess their added value. This product is then used to bias-correct climate projections  
51 from the Canadian Centre for Climate Modelling and Analysis Canadian Regional Climate Model

52 (CanRCM4) between 1950 – 2100 under RCP8.5, and an analysis of the datasets shows that the biases in  
53 the original WFDEI product have been removed and the climate change signals in CanRCM4 are preserved.  
54 The resulting bias-corrected datasets are a consistent set of historical and climate projection data suitable  
55 for large-scale modelling and future climate scenario analysis. The final historical product (WFDEI-GEM-  
56 CaPA, 1979-2016) is freely available at the Federated Research Data Repository at  
57 <http://dx.doi.org/10.20383/101.0111> (Asong et al., 2018) while the original and corrected CanRCM4 data  
58 are available at <https://doi.org/10.20383/101.0162> (Asong et al., 2019).

59 **Subject Keywords:** cold regions processes, observations, bias correction, Mackenzie River Basin

60

61

62

63

64

65

66

67

68

69

70

71

72

73

74 **1 Introduction**

75 Accurate and reliable weather and climate information at the basin scale is in increasingly high  
76 demand by policy-makers, scientists, and other stakeholders for many purposes including water resources  
77 management (Barnett et al., 2005), infrastructure planning (Brody et al., 2007), and ecosystem modelling  
78 (IPCC, 2013). Specifically, the potential impacts of a warming climate on water availability in snow-  
79 dominated high latitude regions continue to be a serious concern given that over the past several decades,  
80 these regions have experienced some of the most rapid warming on earth (Demaria et al., 2016;  
81 Diffenbaugh et al., 2012; Islam et al., 2017; Martin and Etchevers, 2005; Stocker et al., 2013). The on-going  
82 science suggests that these warming trends are resulting in the intensification of the hydrologic cycle,  
83 leading to significant recent observed changes in the hydro-climatic regimes of major river basins in  
84 Canada and globally (Coopersmith et al., 2014; DeBeer et al., 2016; Dumanski et al., 2015). Changes in the  
85 timing and magnitude of river discharge (Dibike et al., 2016), shifts in extreme temperature and  
86 precipitation regimes (Asong et al., 2016b; Vincent et al., 2015) and changes in snow, ice, and permafrost  
87 regimes are anticipated (IPCC, 2013). Substantial evidence also indicates that the long-held notion of  
88 stationarity of hydrological processes is becoming invalid in a changing climate. As pointed out by Milly  
89 et al. (2008), this loss of stationarity means that there will be an increase in the likelihood and frequency  
90 of extreme weather and climate events, including floods and droughts. What is particularly troubling is  
91 that these impacted regions typically have extremely low density of weather and climate observations,  
92 making any attribution and climate impact analysis on water resources difficult.

93 It is well understood that water resources in most watersheds north of 30° N are heavily  
94 dependent on natural water storage provided by snowpacks and glaciers, with water accumulated in the  
95 solid phase during the cold season and released in the liquid phase during warm events and the warm  
96 season. Particularly, the Canadian Rocky Mountains, the hydrological apex of North America with  
97 headwater streams flowing to the Arctic, Atlantic and Pacific oceans, constitutes an integral part of the

98 global hydrological cycle (Fang et al., 2013). Flows in these high elevation headwaters depend heavily on  
99 meltwater from snowpacks and glaciers. However, given that it is characterized by a highly varying cold  
100 region hydroclimate, studies indicate that it is in these high elevation regions where climate variability  
101 and change is expected to be most pronounced in terms of its impacts on water supply (Beniston, 2003;  
102 Kane et al., 1991; Prowse and Beltaos, 2002; Woo and Pomeroy, 2011). More physically realistic and  
103 sophisticated hydrological models driven by reliable climate forcing information can enhance our ability  
104 to assess short- and long-term regional hydrologic responses to increasing variability and uncertainty in  
105 hydro-climatic conditions in a changing climate. Nonetheless, hydrological processes in cold regions  
106 involve complex phase changes and so are very sensitive to small biases in the driving meteorology,  
107 particularly in temperature and precipitation.

108         As described earlier, cold regions often have sparse surface observations, particularly at the high  
109 elevations and high latitudes regions that could potentially generate a major amount of runoff. The effects  
110 of mountain topography and high latitudes are currently not well reflected in the observational record.  
111 Ground-based measurements (e.g. gauges) are limited especially over the Canadian Rocky Mountains,  
112 and suffer from inaccuracies associated with cold climate processes (Asong et al., 2017a; Wang and Lin,  
113 2015; Wong et al., 2017). The advent and use of weather radar systems have addressed some of the  
114 shortcomings of gauge coverage, at least where radar exists. Unfortunately, in Canada, for example, the  
115 spatial coverage of weather radar is limited to the southern (south of 55° N) part of the country (Fortin et  
116 al., 2015b). Recently, improved satellite products have emerged such as the Global Precipitation  
117 Measurement (GPM) mission that provides meteorological information at fine spatiotemporal resolutions  
118 and regular intervals. But, the GPM is still at an early stage of development and only covers the region  
119 south of 60° N (Asong et al., 2017a; Hou et al., 2014).

120         The capability of the current generation of Earth System Models (ESMs) to represent  
121 meteorological forcing variables is therefore of major interest for hydrological climate change impact

122 studies in cold regions watersheds. Despite commendable progress being made, raw outputs from  
123 regional and global ESMs still have large differences between models and from the limited observational  
124 reference meteorology, due partly to spatial scale mismatches and systematic biases (Taylor et al., 2012).  
125 Therefore, ESM outputs are often downscaled and biases are adjusted statistically before being used in  
126 hydrological simulations (Asong et al., 2016b; Chen et al., 2013; Chen et al., 2018; Gudmundsson et al.,  
127 2012). Recent research has demonstrated that bias correction, including adjustment of the dependence  
128 between driving variables, can lead to more realistic hydrological simulations in cold regions watersheds  
129 where the response of the system is sensitive to accumulation and melt of snow and ice (Meyer et al.,  
130 2019).

131         Apart from the uncertainty due to the many empirical statistical techniques which have been  
132 developed to post-process ESM outputs (Maraun, 2016), the quality and length of the reference  
133 observational dataset for bias correction remains a major issue (Reiter et al., 2016; Schoetter et al., 2012;  
134 Sippel et al., 2016). In Canada and other regions of North America, regional gridded datasets such as the  
135 combined Global Environmental Multiscale (GEM) atmospheric model forecasts (Yeh et al., 2002) and the  
136 Canadian Precipitation Analysis—CaPA (Mahfouf et al., 2007) have been found to perform comparably to  
137 ground observations, both statistically and hydrologically (Alavi et al., 2016; Boluwade et al., 2018; Eum  
138 et al., 2014; Fortin et al., 2015a; Gbambie et al., 2017; Wong et al., 2017). However, the duration of GEM-  
139 CaPA is too short to be used to directly correct ESM climate due to unsynchronized internal  
140 variability—the recommended minimum record length for bias correction is 30 years (Maraun, 2016;  
141 Maraun et al., 2017). Other gridded products such as the EU WATCH ERA-Interim reanalysis—WFDEI  
142 (Weedon et al., 2014) and Princeton (Sheffield et al., 2006) have a longer historical record, but have been  
143 found to be biased relative to observations over Canada (Wong et al., 2017) and the United States (Behnke  
144 et al., 2016; Sapiano and Arkin, 2009). However, the WFDEI reanalysis has been found to outperform other  
145 long-record gridded products (Chadburn et al., 2015; Park et al., 2016; Wong et al., 2017).

146           Because of the sparse observational network, few gridded climate datasets exist that contain the  
147 necessary meteorological variables to drive physically-based land surface models at sub-daily temporal  
148 resolution north of 55° N in North America. Because the combination of the GEM and CaPA datasets has  
149 been shown to perform relatively well in these regions, the intent here is to use these datasets to bias-  
150 correct the WFDEI dataset, which contains a sufficient length of record for bias-correcting climate  
151 projection datasets. Aside from its short record length, a limitation of the GEM-CaPA dataset for wider  
152 use for hydrological models is that the wind, temperature, and humidity variables are available only at  
153 the 0.995 sigma( $\sigma$ ) level (approximately 40 m, varying in time and space; herein referred to as the “40 m”  
154 level) across the full length of record. The WFDEI dataset contains these variables at the surface level,  
155 which is more typically used by hydrological models. Therefore, the bias correction effectively modifies  
156 the source surface level data to reproduce the climate found at the 40 m level of the reference dataset  
157 (GEM-CaPA). Many regional and large-scale land surface hydrological models are capable of using climate  
158 data at this atmospheric level. Thus, no effort is made to interpolate the product back to surface level  
159 (although this could be done if needed). In addition, the bias-corrected dataset at an effective 40 m level  
160 can then be used to bias-correct these same fields from the CanRCM4 dataset, which are at the same  
161 0.995  $\sigma$  level as in the reference dataset (GEM-CaPA). The analysis results in a bias-corrected set of  
162 historical and projected climate data that is consistent in time and considers the regional topography and  
163 climate effects of GEM and CaPA, and is suitable to drive large-scale simulations of distributed hydrological  
164 models for assessing climate change impacts in data sparse regions.

165           The aim of this study, therefore, is to combine the strengths of both datasets (GEM-CaPA and  
166 WFDEI) to produce a less-biased long record product (WFDEI-GEM-CaPA) using a multi-stage bias  
167 correction framework. First, a multivariate generalization of the quantile mapping technique was  
168 implemented to bias-correct WFDEI against GEM-CaPA at  $3\text{h} \times 0.125^\circ$  resolution during the 2005-2016  
169 period, followed by a hindcast of WFDEI-GEM-CaPA from 1979. Subsequently, a 15-member initial

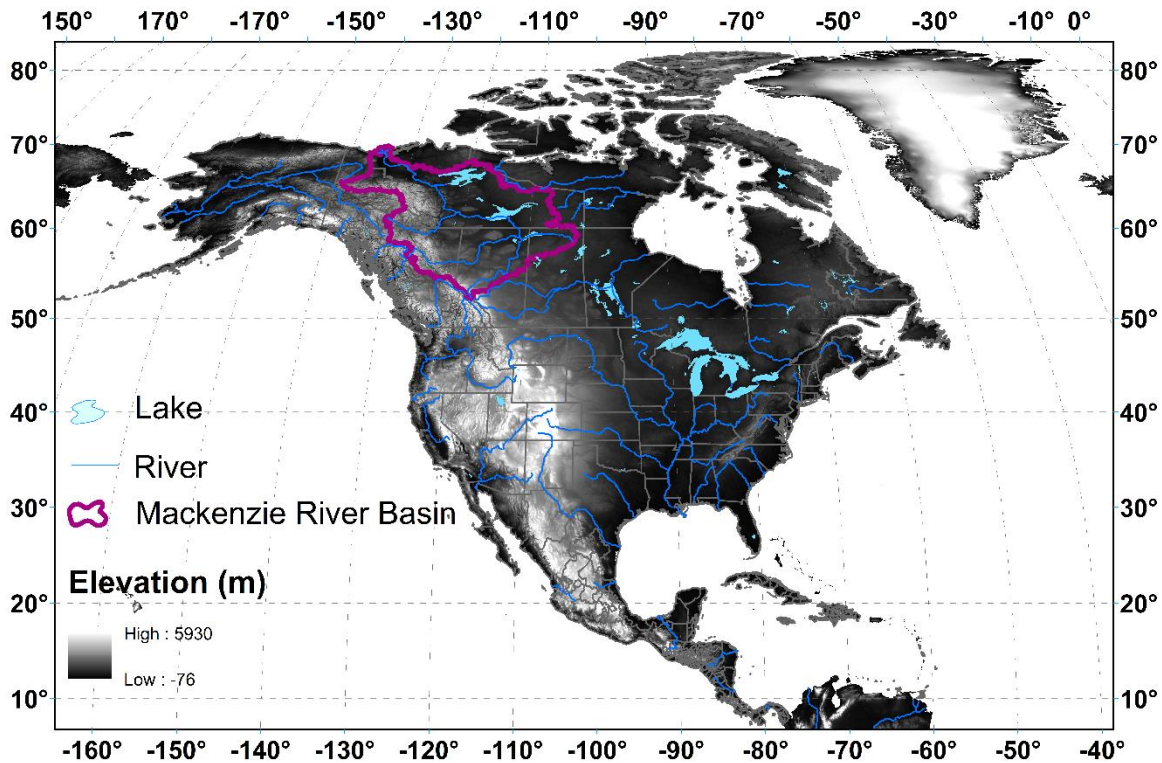
170 condition ensemble of the CanESM2 ESM (historical followed by RCP8.5 scenario), which has been  
171 dynamically downscaled at 0.44° (50 km) resolution using the fourth generation Canadian Regional  
172 Climate Model (CanRCM4), is sourced from the Canadian Centre for Climate Modelling and Analysis. A  
173 multivariate bias correction algorithm is applied to the CanRCM4 outputs (1950 – 2100) to adjust the data  
174 against WFDEI-GEM-CaPA. The bias-corrected products are important for developing distributed  
175 hydrological models as well as for assessing climate change impacts over the Mackenzie River basin (MRB),  
176 which constitutes a testbed for the Changing Cold regions Network (CCRN) project's large-scale  
177 hydrological modelling strategy and is the case study for the current analysis.

## 178 **2 Methodology**

### 179 **2.1 Study area**

180 The study area is the Mackenzie River Basin (MRB), which is the largest river basin in Canada and the  
181 largest river draining from North America to the Arctic Ocean (  
182 **Fig. 1**). It drains an area of about 1.8 million km<sup>2</sup> and discharges more than 300 km<sup>3</sup> of freshwater  
183 to the Beaufort Sea in the Arctic each year. The basin drains parts of British Columbia, Alberta,  
184 Saskatchewan, the Northwest Territories and the Yukon Territory in northwestern Canada. The western  
185 tributaries are relatively steep as they originate from the Canadian Rocky Mountains while the eastern  
186 tributaries have milder topography with several large lakes, thousands of interconnected small lakes, fens  
187 and bogs. The general vegetation ranges widely between alpine, boreal and tundra landscapes. Climatic  
188 conditions are also quite variable and can be generally classified as cold-temperate, mountain, subarctic  
189 and arctic zones, with about 75% of the basin underlain by continuous and discontinuous permafrost.





190  
191  
192

**Fig. 1:** Location of the Mackenzie River Basin in North America

193 **2.2 Data sources**

194 **2.2.1 Gridded GEM-CaPA product**

195 Hourly archived forecast data from the GEM model were acquired from Environment and Climate  
 196 Change Canada ([http://collaboration.cmc.ec.gc.ca/cmc/cmci/product\\_guide/submenus/rdps\\_e.html](http://collaboration.cmc.ec.gc.ca/cmc/cmci/product_guide/submenus/rdps_e.html),  
 197 last access: 28 September 2018). The fields include downward incoming solar radiation, downward  
 198 incoming longwave radiation and pressure at the surface, as well as specific humidity, air temperature,  
 199 and wind speed at approximately 40 m above ground surface. The 40 m level was used because surface  
 200 level variables at  $1.0 \sigma$  (approximately at 2 m for temperature and humidity, and 10 m for wind speed)  
 201 are only available in the archive from 2010 onward. The GEM data are at approximately 24 km spatial  
 202 resolution from October 2001, approximately 15 km from June 2004, and approximately 10 km resolution  
 203 from November 2012, and are provided on a rotated latitude/longitude grid in Environment and Climate

204 Change Canada (ECCC) ‘standard file’ format. The archived data are of former operational forecasts and  
205 contain model outputs from versions of GEM prior to 2.0.0 through 5.0.0.

206 6-Hourly total precipitation data from the complementary CaPA product  
207 ([http://collaboration.cmc.ec.gc.ca/cmc/cmoi/product\\_guide/submenus/capa\\_e.html](http://collaboration.cmc.ec.gc.ca/cmc/cmoi/product_guide/submenus/capa_e.html), last access: 28  
208 September 2018) were also acquired. The analysis incorporates observed precipitation from  
209 meteorological weather stations, and more recently from radar, into the precipitation field from GEM.  
210 The CaPA data are approximately 10-km resolution from January 2002, also on a rotated  
211 latitude/longitude grid in ECCC ‘standard file’ format. The data contain reanalysis outputs from CaPA  
212 2.4b8 from 2002-2012, and of former operational analyses from versions of CaPA 2.3.0 through 4.0.0 from  
213 November 2012 onward.

214 The variables from GEM and CaPA were spatially interpolated and re-projected to a regular  
215 latitude/longitude grid at 0.125° resolution. For data from GEM, the interpolation was done using a  
216 bilinear algorithm, while data from CaPA were interpolated using nearest neighbor (Schulzweida et al.,  
217 2004). Where necessary, the GEM fields were converted to SI units and CaPA was converted to a  
218 precipitation rate in SI units for better compatibility with some hydrological models.

### 219 **2.2.2 Gridded WFDEI product**

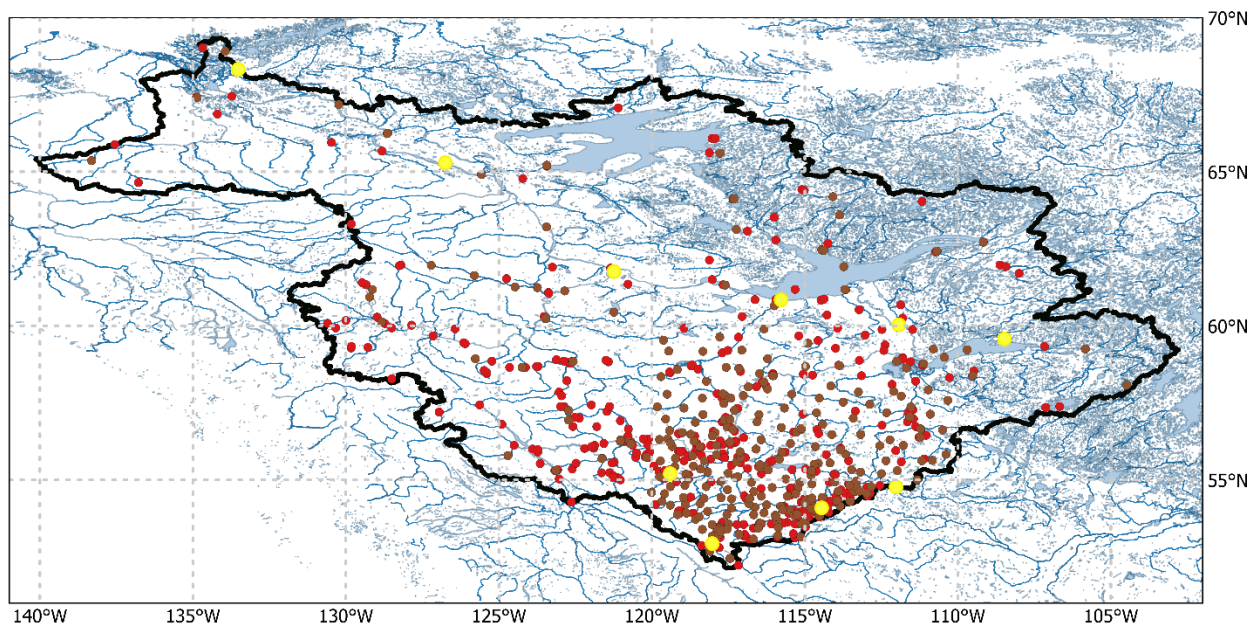
220 The gridded WFDEI meteorological forcing data has a global 0.5° spatial resolution and 3-h time  
221 step covering the period 1979-2016 ([http://www.eu-watch.org/data\\_availability](http://www.eu-watch.org/data_availability), last access: 25 July  
222 2018). Weedon et al. (2014) used the ERA-Interim surface meteorology data as baseline information to  
223 derive the WFDEI product. Firstly, ERA-Interim data were interpolated at half-degree spatial resolution to  
224 match the land–sea mask defined by the Climatic Research Unit (CRU) of the University of East Anglia,  
225 Norwich, England. Subsequently, corrections for elevation and monthly bias of climate trends in the ERA-  
226 Interim fields were applied to the interpolated data. The WFDEI data have two sets of precipitation data:  
227 the Global Precipitation Climatology Centre product (GPCC) and CRU Time Series version 3.1 (CRU TS3.1).

228 Thus, two variants of the WFDEI product are available—WFDEI-GPCC and WFDEI-CRU. The WFDEI-CRU  
229 dataset was used here because it goes up to 2016, whilst the WFDEI-GPCC had only been updated until  
230 2013 at the time of our analysis.

### 231 **2.2.3 Station observations**

232 To evaluate the added value of bias-correcting WFDEI against GEM-CaPA, *in situ* hourly  
233 precipitation, temperature, surface pressure, relative humidity, and wind speed at 773 stations located  
234 across the MRB were initially considered (**Fig. 2**). This station network is maintained by Environment and  
235 Climate Change Canada (ECCC) ([http://climate.weather.gc.ca/historical\\_data/search\\_historic](http://climate.weather.gc.ca/historical_data/search_historic_data_e.html)  
236 [data\\_e.html](http://climate.weather.gc.ca/historical_data/search_historic_data_e.html), last access: 17 December 2019) and includes some duplicate stations (stations at the same  
237 location but having different IDs). Total daily precipitation and average daily temperature are found in  
238 daily data files while surface pressure, relative humidity, and wind speed are only found in hourly files.  
239 Unfortunately, radiation data are not available at any of those stations. The data were extracted for the  
240 period from 01 January 2005 to 31 December 2016 and hourly data were averaged to the daily time step.  
241 This reduced the number of stations to 364. Out of these 364 stations, only 10 were found to have less  
242 than 10% missing data (calculated at the daily timescale after aggregating/averaging the data) for all  
243 studied variables concurrently over the 2005-2016 period and were retained for further consideration.  
244 Precipitation and surface pressure are the only two surface variables in all datasets (gridded and stations).  
245 Due to differences in heights between gridded variables of GEM-CaPA and WFDEI-GEM-CaPA datasets for  
246 air temperature, humidity, and wind speed (see Sections 2.2.1 and 3.1) and the ECCC station data, we  
247 expect deviations. Nevertheless, the comparisons are still informative. Relative humidity observations  
248 were converted to specific humidity to be comparable to gridded datasets using concurrent station  
249 temperature and surface pressure data at those stations, which reduced the record completeness further  
250 but was still within 90% for the 10 selected stations. **Table 1** provides additional information for the 10  
251 stations retained for further analysis, which are highlighted in **Fig. 2**. This dataset is hereafter referred to

252 as ECCC-S (S for stations). Table S1 in the Supplementary material provides a similar listing to **Table 1** but  
 253 for all 364 stations with records during the 2005-2016 period.



254  
 255 **Fig. 2:** Spatial distribution of the initial 773 ground-based precipitation gauges (all dots) over the study  
 256 area. Only 364 of these have during the period 2005 – 2016 (brown & yellow dots). Data screening for  
 257 missing values (10% threshold concurrently applied for all variables) during the 2005-2016 period  
 258 resulted in 10 of these stations (yellow dots) being retained for validation of gridded datasets.

259

260 **Table 1:** List of observation stations used for validating the various gridded historical products

Name	Prov.	Station	Coordinates			Record			% Complete			
		ID	Lat	Long	Elev.	Start	End	T	P	RH	ps	wind
JASPER WARDEN	AB	10223	52.93	-118.03	1020.0	1994	2019	99.0	98.0	96.0	96.9	97.1
BEAVERLODGE RCS	AB	30669	55.20	-119.40	745.0	2001	2019	99.0	93.9	93.8	93.9	93.8
BARRHEAD CS	AB	30641	54.09	-114.45	648.0	2000	2019	98.2	98.1	97.8	97.8	97.0
LAC LA BICHE CLIMATE	AB	30726	54.77	-112.02	567.0	2001	2019	99.0	98.8	97.8	97.9	97.9
URANIUM CITY (AUT)	SK	9831	59.57	-108.48	318.2	1992	2019	95.8	93.0	94.2	94.4	94.8
NORMAN WELLS CLIMATE	NT	43004	65.29	-126.75	93.6	2003	2019	98.5	96.6	96.0	95.4	96.2
FORT SMITH CLIMATE	NT	41884	60.03	-111.93	203.0	2003	2019	97.6	96.8	95.8	96.7	97.3
HAY RIVER CLIMATE	NT	41885	60.84	-115.78	164.0	2003	2019	99.6	99.3	98.4	98.4	98.0
FORT SIMPSON CLIMATE	NT	41944	61.76	-121.24	168.0	2003	2019	97.5	99.5	96.1	96.2	98.2
INUVIK CLIMATE	NT	41883	68.32	-133.52	103.0	2003	2019	99.6	95.1	98.3	98.4	97.0

261

## 262 2.2.4 Climate model outputs

263 The historical and future climate simulations utilized in this study are part of the CanRCM4 large  
264 ensemble, which consists of 50 members and downscaled at horizontal spatial resolutions of 0.44° (~50  
265 km). These CanRCM4 simulations had been produced initially by the Canadian Sea Ice and Snow Evolution  
266 Network (CanSISE) Climate Change and Atmospheric Research (CCAR) Network project  
267 (<https://www.cansise.ca/>, last access: 24 April 2019). The input data for the historical period, i.e., 1950 –  
268 2005 as well as the future (2006 – 2100) RCP simulations of CanRCM4 were provided by the parent ESM  
269 (CanESM2) as specified in the Coupled Model Intercomparison Project Phase 5 (CMIP5) guidelines. The  
270 data are sourced from the Canadian Centre for Climate Modelling and Analysis (CCCma) at  
271 [www.cccma.ec.gc.ca/data/canrcm/CanRCM4](http://www.cccma.ec.gc.ca/data/canrcm/CanRCM4) (last access: 6 March 2019). This study utilized 15 members  
272 of the 0.44° resolution product at 1-h time step and values were aggregated to 3-h resolution prior to bias  
273 correction. The seven forcing variables needed for driving the CCRN MESH model  
274 (<https://wiki.usask.ca/display/MESH/About+MESH>, last access: 10 May 2019) and which were bias-  
275 corrected in the current study are included in **Table 2**.

276 **Table 2:** List of variables processed in this study with heights and units in each dataset

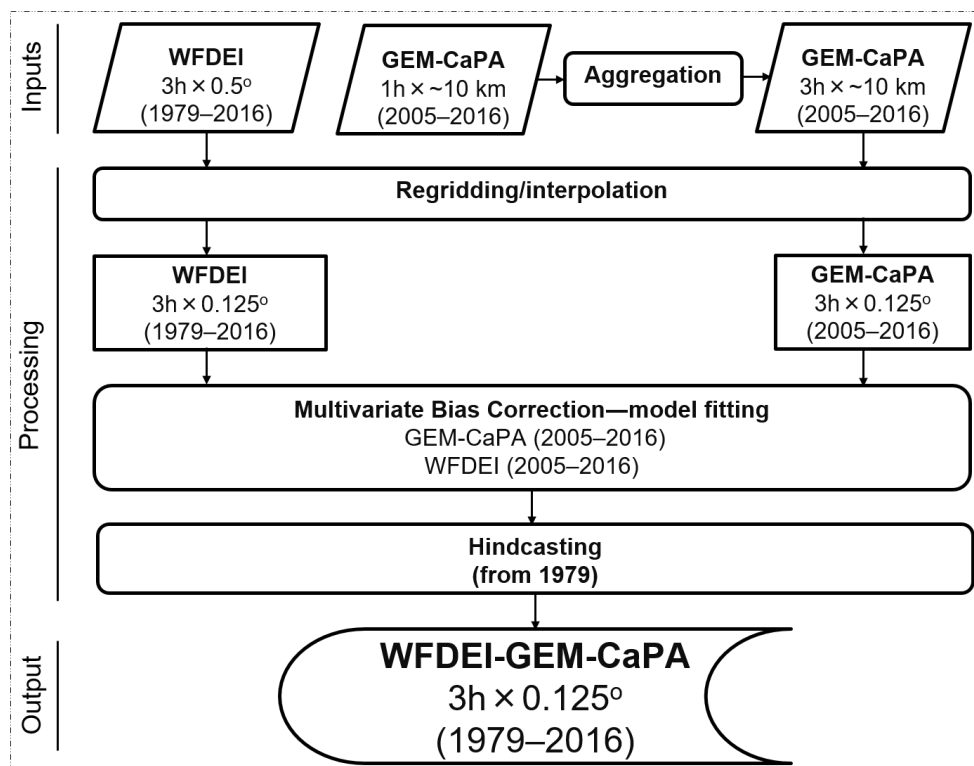
Variable	Unit	Height		
		WFDEI	GEM-CaPA	WFDEI-GEM-CaPA
Precipitation	kg m <sup>-2</sup> s <sup>-1</sup>	Surface	Surface	Surface
Air Temperature	K	2 m	40 m	40 m
Specific Humidity	kg kg <sup>-1</sup>	2 m	40 m	40 m
Wind Speed	m s <sup>-1</sup>	10 m	40 m	40 m
Surface Pressure	Pa	Surface	Surface	Surface
Downwelling Shortwave Radiation	W m <sup>-2</sup>	Surface	Surface	Surface
Downwelling Longwave Radiation	W m <sup>-2</sup>	Surface	Surface	Surface

277

## 278 2.3 Data processing and bias correction workflow

279 The workflow for the multi-stage bias correction of WFDEI against GEM-CaPA is shown in **Fig. 3**.  
280 Bias correction was done after aggregating 1-h GEM-CaPA estimates to 3-h (the values at each time step  
281 represent the mean of the previous 3-h period, to make it consistent with WFDEI) and interpolating both

282 WFDEI and GEM-CaPA to  $0.125^\circ$  resolution. For bias correction, a multi-stage approach was implemented  
 283 as follows. A multivariate generalization of the quantile mapping technique (MBCn, Cannon, 2018) which  
 284 combines quantile delta mapping (Cannon et al., 2015) and random orthogonal rotations to match the  
 285 multivariate distributions of two datasets was implemented to bias-correct WFDEI against GEM-CaPA at  
 286  $3\text{-h} \times 0.125^\circ$  resolution during the 2005-2016 period. The rationale for selecting the above bias correction  
 287 method is based on fitness for purpose, i.e. the method accounts for dependence between variables and  
 288 corrects multiple measures of joint dependence — attributes that can be important for hydrological  
 289 simulations (Meyer et al., 2019) — to preserve the physical realism of the corrected climate as much as  
 290 possible. Models were fitted to data for each calendar month while accounting for inter-variable  
 291 dependence structure. Using the fitted models (2005-2016), a hindcast was made of WFDEI between  
 292 1979-2004. Finally, the corrected WFDEI data derived from the fitted (2005-2016) and hindcast (1979-  
 293 2004) periods were concatenated to obtain the bias-corrected WFDEI-GEM-CaPA product (1979-2016).



294  
 295  
 296

**Fig. 3:** A schematic representation of inputs and bias correction procedure used to produce the WFDEI-GEM-CaPA meteorological forcing dataset

297 For bias-correcting the 15-member CanRCM4 initial condition ensemble against the WFDEI-GEM-  
298 CaPA product, CanRCM4 was also spatially interpolated to match the WFDEI-GEM-CaPA specifications  
299 using nearest neighbor interpolation. The multivariate bias correction technique (described above)  
300 transfers all aspects of the WFDEI-GEM-CaPA continuous multivariate distribution to the corresponding  
301 multivariate distribution of variables from CanRCM4 during the 1979 – 2008 calibration period (also used  
302 here as historical period). Subsequently, when applied to future projections, changes in quantiles of each  
303 variable between the historical and future period are also preserved. Models were fitted to data for each  
304 calendar month and for each grid point while preserving the dependence structure among variables. The  
305 historical datasets used in the fitting procedure include WFDEI-GEM-CaPA (1979 – 2008) and CanRCM4  
306 (1979 – 2008). Using the fitted models, quantiles of CanRCM4 output from 1950 – 2100 were changed. To  
307 evaluate the need to bias-correct CanRCM4, performance of the bias correction scheme, as well the  
308 impact of bias correction on the climate change signal, the seasonal cycle of all 7 variables is assessed over  
309 three 30-year periods: 1979–2008 (referred hereafter as 1990s); 2021–2050 (referred to hereafter as  
310 2030s) and 2071–2100 (referred to hereafter as 2080s).

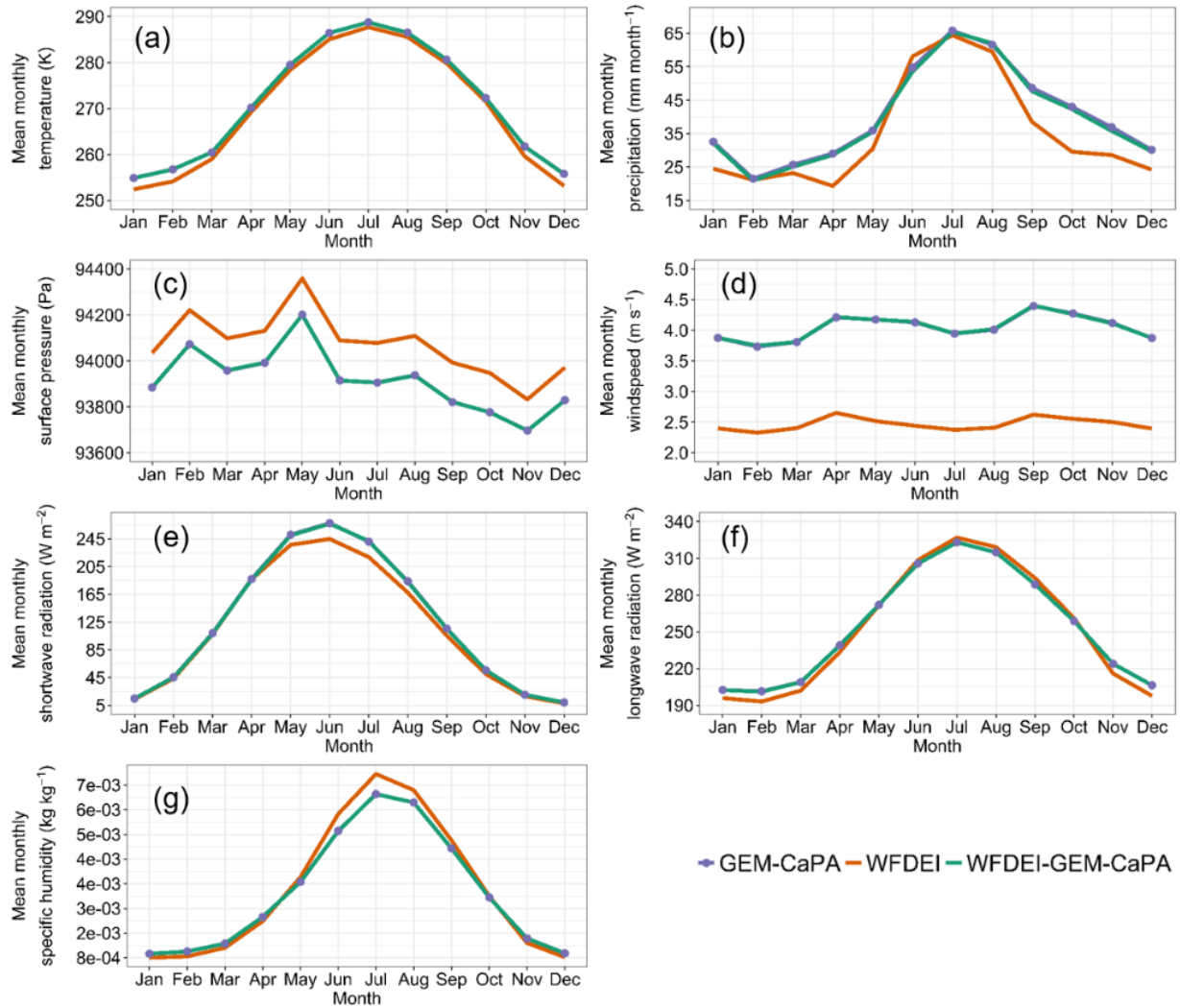
### 311 **3 Results and discussion**

#### 312 **3.1 Bias correction of WFDEI**

313 Table 2 presents an overview of the seven variables processed in this study. Note that three of  
314 the GEM variables (temperature, specific humidity, and wind speed) are at 40 m and are used directly to  
315 correct the corresponding WFDEI surface variables (see **Table 2**). Therefore, the corrected WFDEI-GEM-  
316 CaPA data for those 3 variables reflect 40 m elevations above the surface. The spatial coverage of the  
317 WFDEI-GEM-CaPA data is the same as the areal extent of the MRB (Figs. 1 and 2). The suitability of the  
318 bias correction algorithm to reproduce the observed seasonal cycle and inter-annual variability of the  
319 variables was assessed for the fitting (2005-2016) and hindcast (1979-2004) periods. Data extracted over  
320 the entire Mackenzie River basin is used to demonstrate the quality of the bias correction exercise and

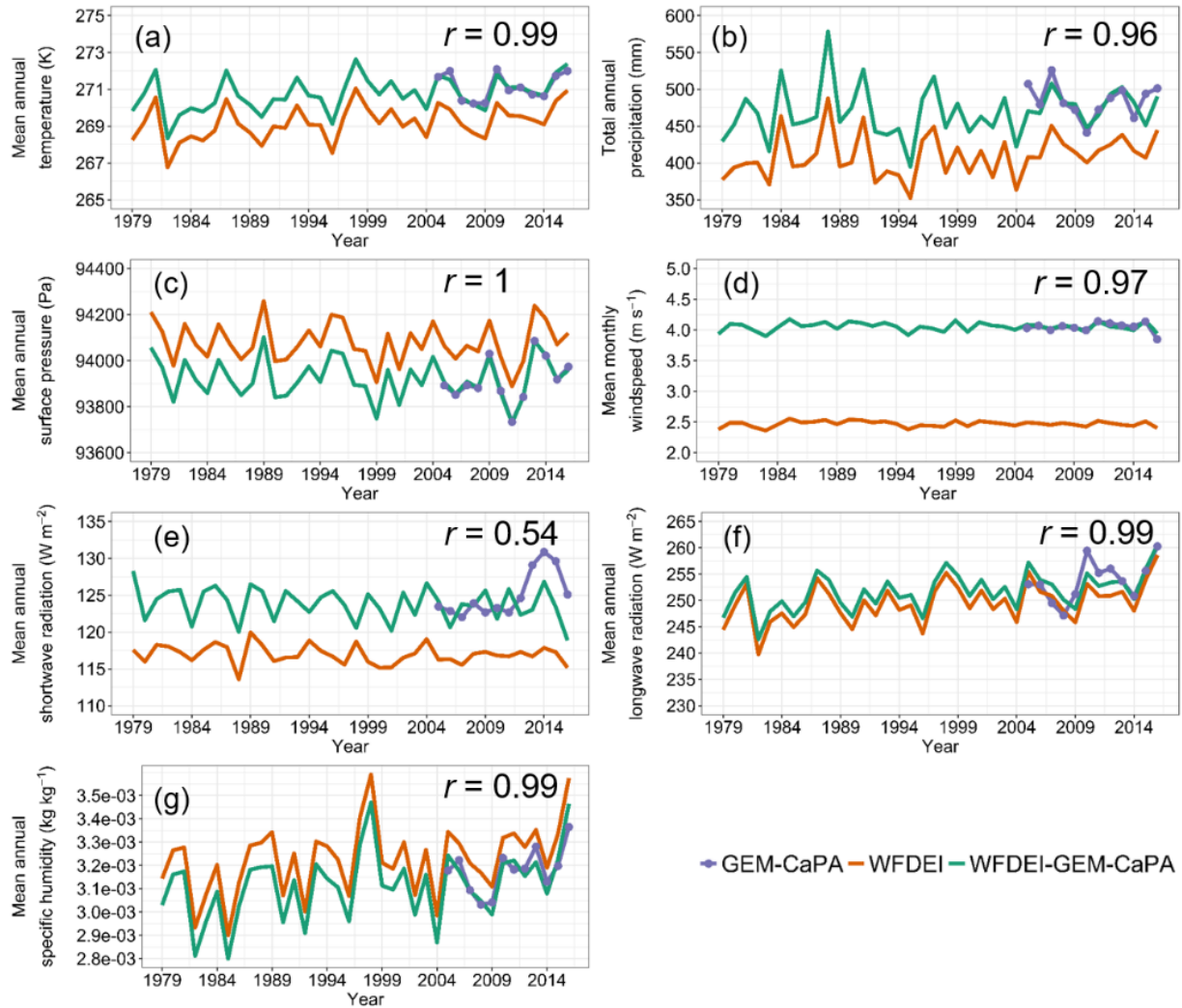
321 uniqueness of the resulting output. **Fig. 4** shows the seasonal cycle for GEM-CaPA, WFDEI and WFDEI-  
322 GEM-CaPA during the fitting period. Overall, the monthly distributions show that the bias was removed  
323 for all variables resulting in the very close distributions between GEM-CaPA and WFDEI-GEM-CaPA. The  
324 bias was particularly large for wind speed, an important variable for both alpine and prairie blowing snow  
325 redistribution calculations (Pomeroy and Li, 2000), but was successfully removed. **Fig. 5** shows the mean  
326 annual time series of the seven variables over the 1979-2016 period. It is noticeable that the bias is  
327 corrected while the inter-annual variability is well preserved between WFDEI and WFDEI-GEM-CAPA,  
328 except for shortwave radiation where the inter-annual variability is not fully preserved as shown by the  
329 correlation between the WFDEI and WFDEI-GEM-CaPA annual series. However, this should not be a major  
330 issue when impact models are driven using these data. The foregoing analyses have shown that the bias  
331 in the WFDEI data was removed for both the fitting and hindcast periods. However, some potential  
332 limitations remain—for example, WFDEI was interpolated directly from 0.5° to 0.125° and bias-corrected  
333 against GEM-CaPA at 0.125°. The interpolation does not add any event-scale spatial variability for a  
334 variable like precipitation which is very variable across different scales. These issues have been reviewed  
335 extensively by Cannon (2018), Maraun (2013), Maraun et al. (2010), and Storch (1999).  
336





337  
 338 **Fig. 4:** Seasonal cycle of GEM-CaPA (dark slate blue), WFDEI (orange) and bias corrected data—WFDEI-  
 339 GEM-CaPA (green) for air temperature (a), precipitation (b), surface pressure (c), wind speed (d),  
 340 shortwave radiation (e), longwave radiation (f), and specific humidity (g) during the fitting period (2005-  
 341 2016)

342



343  
 344 **Fig. 5:** Time series of GEM-CaPA (dark slate blue), WFDEI (orange) and bias corrected data—WFDEI-  
 345 GEM-CaPA (green) for air temperature (a), precipitation (b), surface pressure (c), wind speed (d),  
 346 shortwave radiation (e), longwave radiation (f), and specific humidity (g) during the periods 2005-2016  
 347 (GEM-CaPA) and 1979-2016 (WFDEI and WFDEI-GEM-CaPA). The correlation ( $r$ ) between the WFDEI and  
 348 WFDEI-GEM-CaPA annual series is indicated for each variable.

### 349 3.2 Validation of gridded products against station observations

350 In this section, the WFDEI-GEM-CaPA product is validated against station observations (ECCC-S)  
 351 to indicate the benefit of bias-correcting WFDEI against GEM-CaPA. As mentioned in Section 2.2.3, the  
 352 validation focusses on variables for which station data could be found. Thus, shortwave and longwave  
 353 radiation are not validated as we could not find station data for those in ECCC-S data. The height  
 354 differences for temperature, humidity and wind speed between GEM-CAPA and WFDEI-GEM-CaPA (40 m)  
 355 on one side and ECCC-S data (surface) on the other introduce some inconsistencies that are discussed

356 below. Indirect validation is recommended for other variables through other means such as hydrological  
357 modelling. Validation is performed for the 2005 – 2016 period using daily totals for precipitation and daily  
358 averages for other variables. To compare stations against gridded products, the corresponding time series  
359 of gridded products for each gauge were obtained from the cell that contained the gauge (i.e. nearest  
360 neighbor) and were aggregated to the daily time scale.

361 **Fig. 6** depicts quantile–quantile (Q–Q) plots of daily precipitation from WFDEI-GEM-CaPA, WFDEI  
362 and GEM-CaPA compared against ECCC-S. As expected, although with noticeable differences across the  
363 MRB, CaPA agrees better with ECCC-S than WFDEI since some or all of these meteorological stations are  
364 assimilated by the CaPA system. Large daily amounts are generally underestimated by CaPA but CaPA  
365 sometimes overestimates these as well (e.g. Uranium City (AUT) station). WFDEI tends to underestimate  
366 the observed precipitation amounts at most stations except at Jasper Warden where it slightly  
367 overestimates small and moderate amounts. Bias correction brings WFDEI closer to CaPA for most stations  
368 but some biases remain, especially at the high ends of the distributions.

369 **Fig. 7** shows quantile–quantile (Q–Q) plots of mean daily temperature for the three gridded  
370 datasets versus ECCC-S. WFDEI is performing generally well for temperature except for low temperatures  
371 at Inuvik (the most northerly station). Despite the height difference (see Section 2.2.3), GEM is also close  
372 to observations for most stations with some overestimation of low temperatures. The temperature  
373 differences between the surface and the 40m level are generally small (1-2°C) at the daily scale. Given  
374 that temperature biases in WFDEI were small, WFDEI-GEM-CaPA is almost identical to GEM, i.e. all biases  
375 are removed.

376

377

378

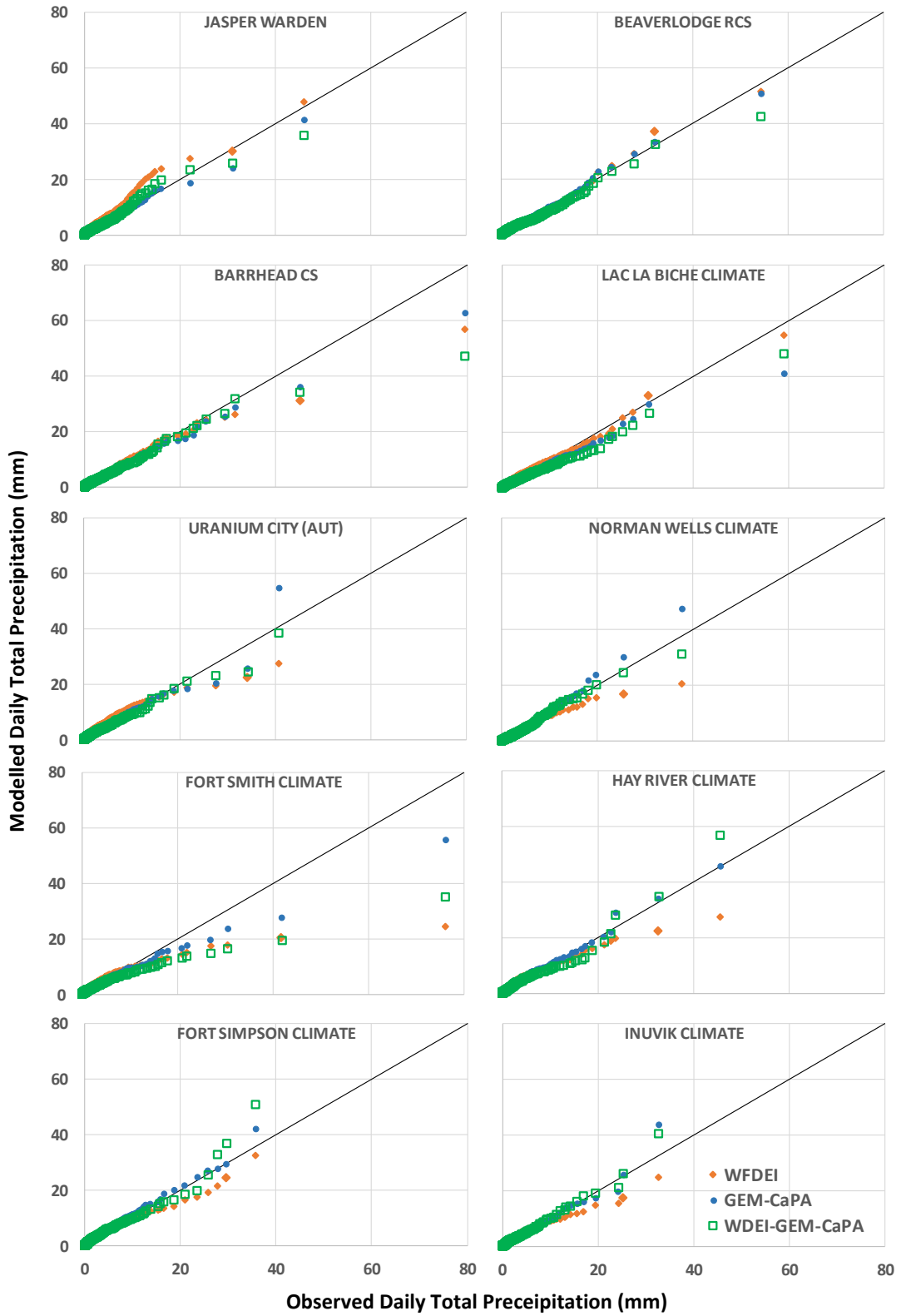
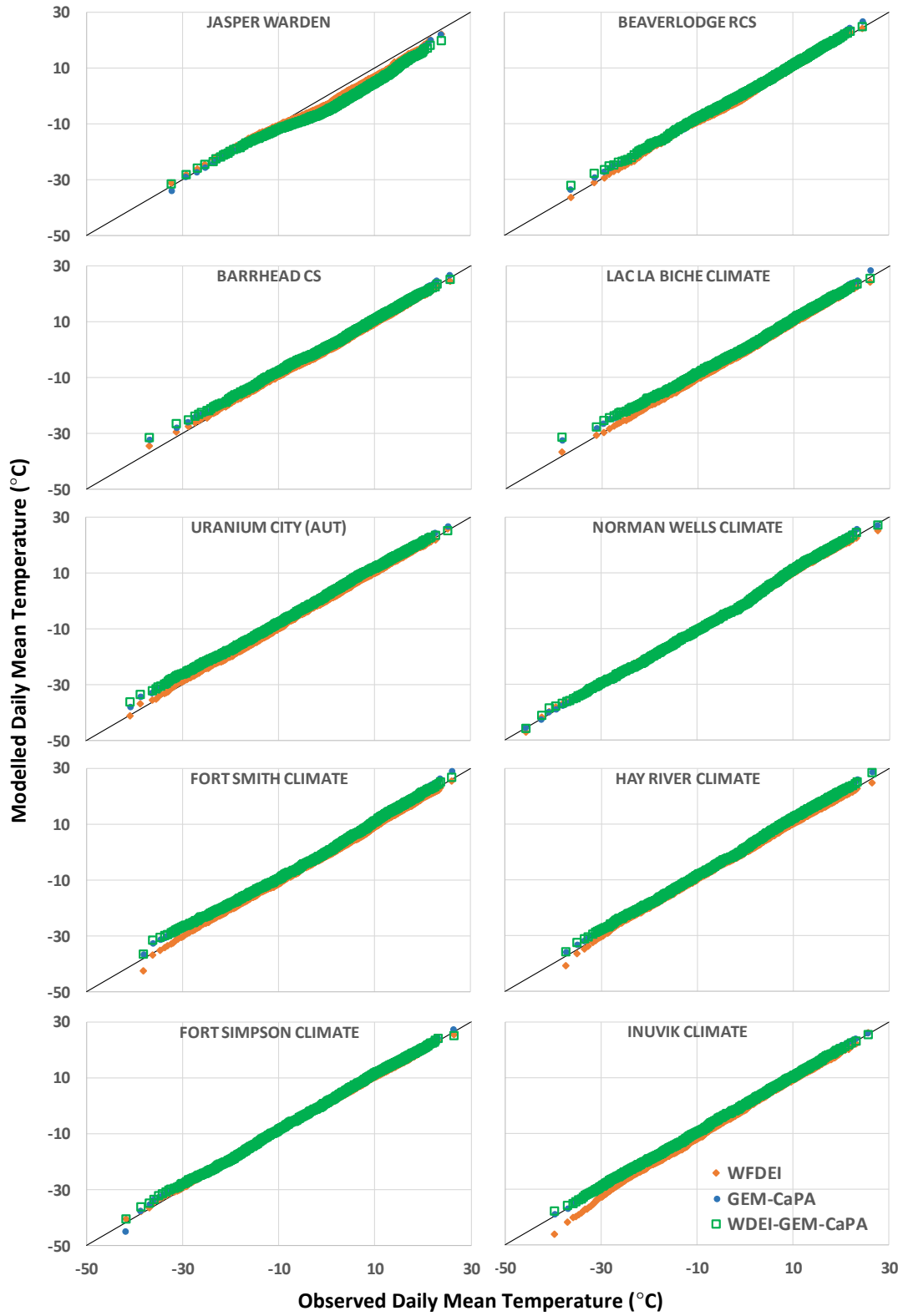


Fig. 6: Quantile-quantile plots of modelled (GEM-CaPA, WFDEI and WFDEI-GEM-CaPA) and observed (ECCC-S) daily total precipitation



**Fig. 7:** Quantile-quantile plots of modelled (GEM-CaPA, WFDEI and WFDEI-GEM-CaPA) and observed (ECCC-S) daily mean temperature

380 Comparisons between gridded datasets and stations for daily mean surface pressure, wind speed,  
381 and humidity are shown in Figs. 8, 9, and 10 respectively. WFDEI is generally performing well for surface  
382 pressure (**Fig. 8**) such that bias correction seems unnecessary at most locations. Both datasets (WFDEI and  
383 GEM) underestimate surface pressure at Jasper Warden station, which is at a relatively high elevation.  
384 GEM is worse than WFDEI for this station and thus bias correction against GEM-CaPA deteriorates the  
385 results. WFDEI slightly underestimates surface pressure at Uranium City (AUT) and Norman Wells Climate  
386 stations but because GEM is close to observations, bias correction makes WFDEI-GEM-CaPA close to  
387 observations at those two stations.

388 Mean daily wind speed (**Fig. 9**) is underestimated by WFDEI for most stations, especially at high  
389 speeds. GEM winds are generally higher (except for Fort Simpson) because of the higher elevation (40 m)  
390 of the dataset and thus the comparison to ECCC-S data is not favorable for this variable. It is generally  
391 expected that wind speed increases with height. Bias correction of WFDEI against GEM-CaPA removes  
392 differences between the two datasets and the resultant wind speed, thus, reflects the higher speeds to  
393 be expected at 40 m.

394 Both WFDEI and GEM are close in terms of specific humidity at most stations (**Fig. 10**) despite the  
395 height difference, with few exceptions. For example, humidity at Jasper Warden, Barrhead CS and Inuvik  
396 Climate is underestimated by both WFDEI and GEM, especially at high values. Bias correction brings WFDEI  
397 closer to GEM and thus results in improvements only if GEM is closer to observations than WFDEI. Thus,  
398 results at Fort Smith Climate and Inuvik Climate stations are worse with bias correction. However, the bias  
399 correction does not change the quantiles by much for most stations.

400

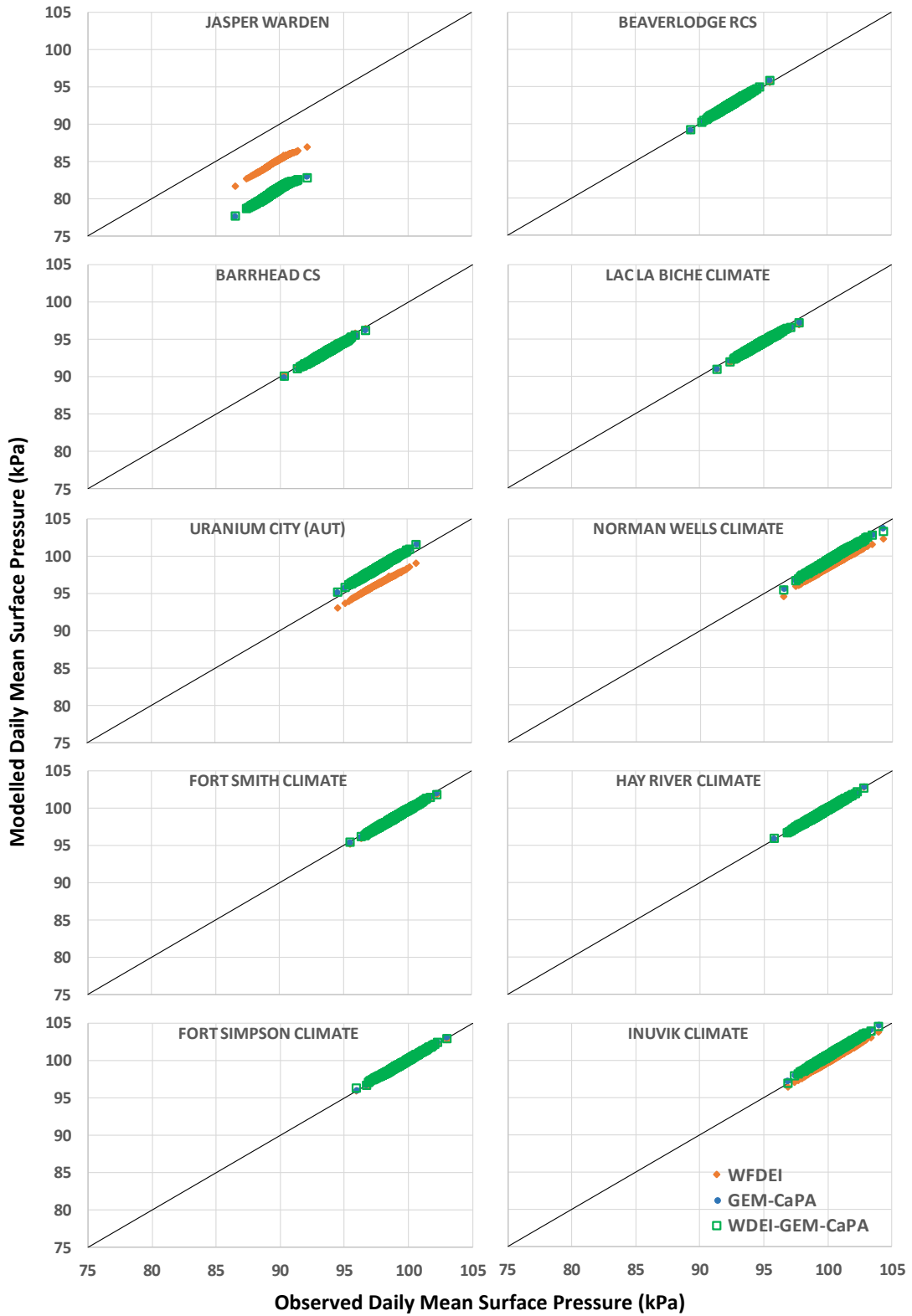


**Fig. 8:** Quantile-quantile plots of modelled (GEM-CaPA, WFDEI and WFDEI-GEM-CaPA) and observed daily mean surface pressure

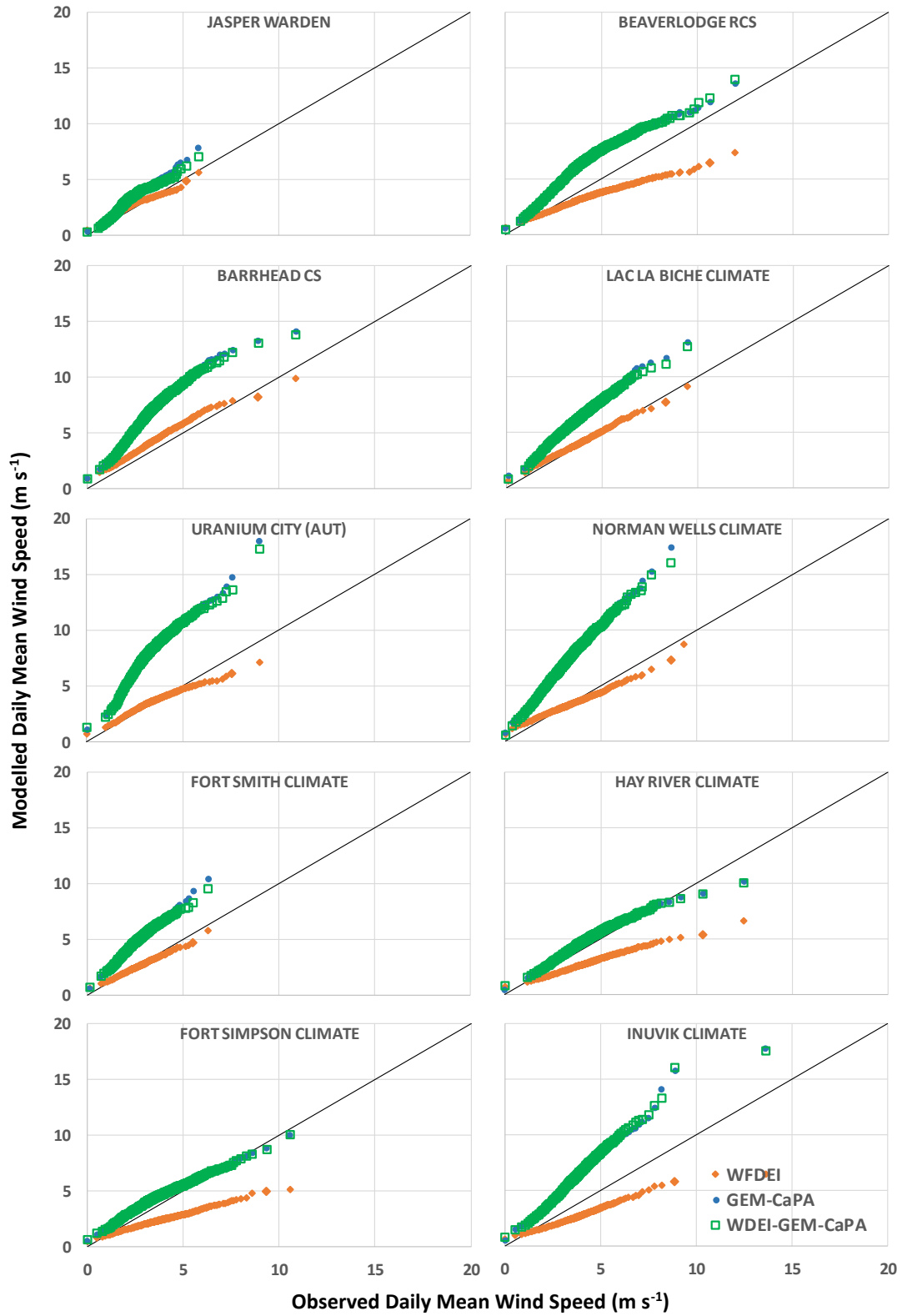


Fig. 9: Quantile-quantile plots of modelled (GEM-CaPA, WFDEI and WFDEI-GEM-CaPA) and observed daily mean wind speed



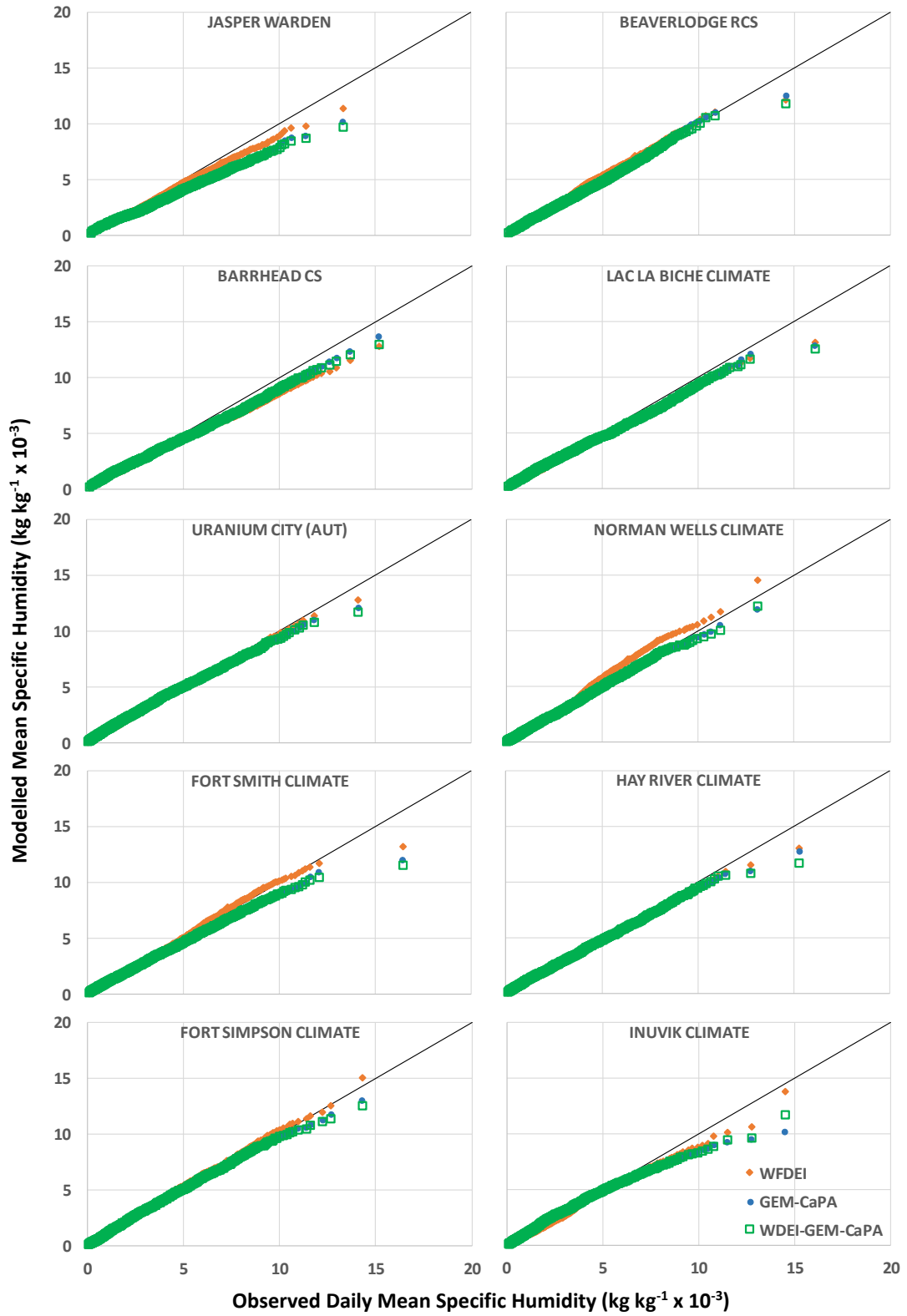


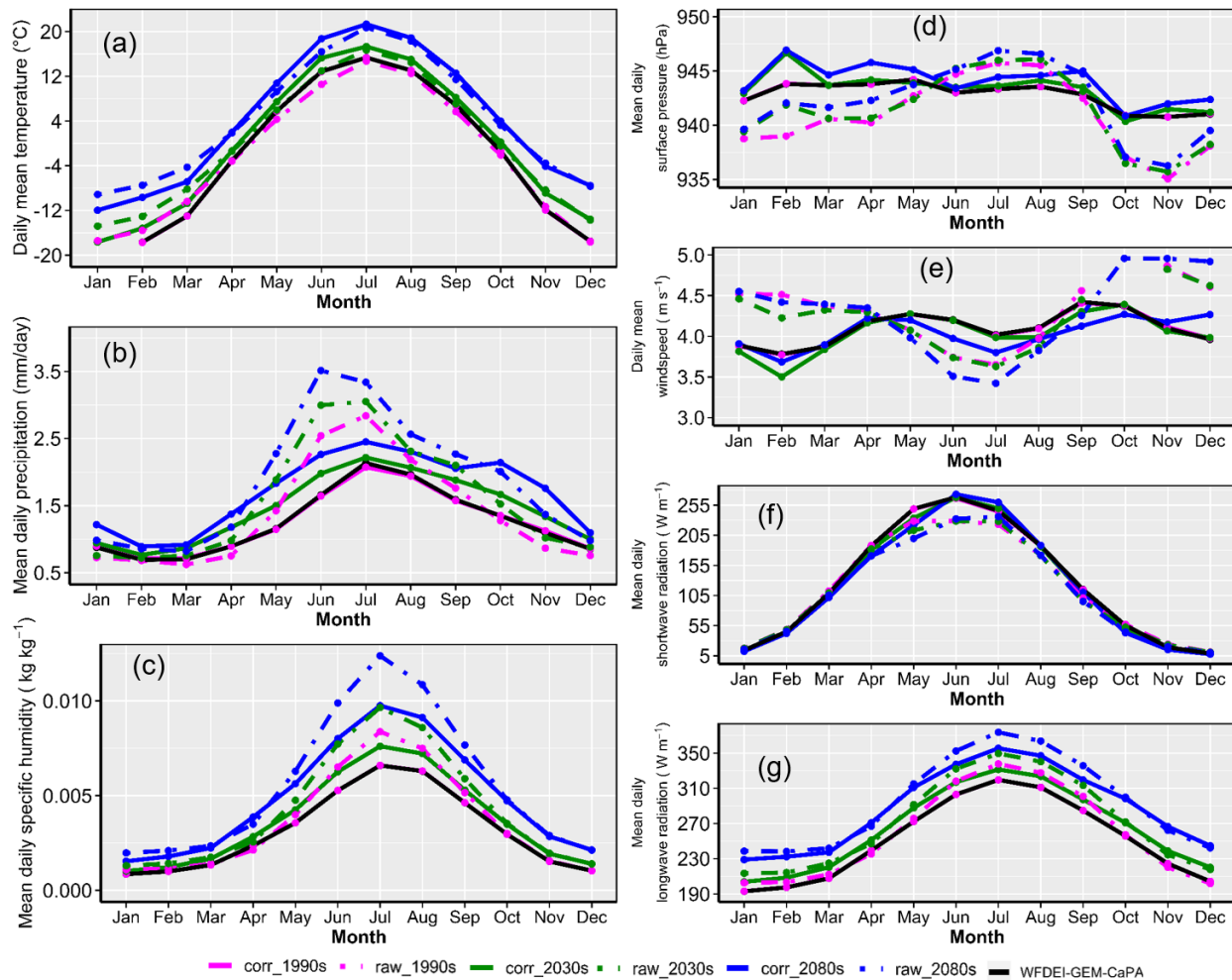
Fig. 10: Quantile-quantile plots of modelled (GEM-CaPA, WFDEI and WFDEI-GEM-CaPA) and observed daily specific humidity

401 Overall, GEM-CaPA performs similar to or better than WFDEI for most variables at the studied  
402 stations, especially precipitation. Therefore, correcting WFDEI against GEM-CaPA adds value to the WFDEI  
403 dataset and leads to a closer agreement between WFDEI-GEM-CaPA and ECCS-S. Precipitation is one of  
404 the most important variables and most difficult to correct. Note that extracting data from grid points does  
405 not only have the effect of smoothing the areal averages but comparing grid point estimates to station  
406 values may not provide a clear picture of the quality of a gridded product. However, this diagnostic  
407 analysis provides preliminary insights into the potential performance of a dataset.

### 408 **3.2 Bias correction of future climate projections**

409 In this section, the need to bias-correct the CanRCM4 outputs is shown and whether the simulated  
410 climate change signal was preserved after applying MBCn to the CanRCM4 outputs is determined. **Fig. 11**  
411 shows the climatological seasonal cycle of all 7 variables which are required to drive the MESH model for  
412 the MRB. First, between April and October, CanRCM4 overestimates the observed (i.e. WFDEI-GEM-CaPA)  
413 daily precipitation amounts and specific humidity during the historical period. This is also true in the case  
414 of daily mean wind speed in the cold months (October to April). However, it underestimates the wind  
415 speed in the warm season (May to September). Surface pressure is underestimated during September to  
416 May and overestimated in the summer (June to August). For the other variables (e.g. air temperature and  
417 radiation), CanRCM4 can simulate the observed seasonal cycle closely although biases still exist. These  
418 biases necessitated the application of the MBCn algorithm on the raw CanRCM4 outputs. The MBCn  
419 algorithm removed the bias in the CanRCM4 simulations during the fitting period (1990s) as can be judged  
420 from the close fit between WFDEI-GEM-CaPA and the unbiased CanRCM4 output (corr\_1990s). On the  
421 projected climate change signal, there is a projected change in the amplitude of all variables but not a  
422 shift in the phase of the cycle over the MRB with global warming. Precipitation, specific humidity and  
423 longwave radiation are projected to increase in the future, with larger changes expected in the warm  
424 season (April – October) while air temperature is projected to increase, particularly in the cold months

425 (October – March). These climate change signals are very well preserved after applying MBCn to the  
 426 CanRCM4 simulations.



427  
 428 **Fig. 11:** Seasonal cycle of WFDEI-GEM-CaPA, raw and bias-corrected CanRCM4 data for air temperature  
 429 (a), precipitation (b), specific humidity (c), surface pressure (d), wind speed (e), shortwave radiation (f),  
 430 and longwave radiation (g) during the periods 1979–2008; 2021–2050 and 2071–2100.

431 **4 Conclusions**

432 Cold regions hydrology is very sensitive to the impacts of climate warming. More physically  
 433 realistic hydrological models need to be driven by reliable climate forcing and can provide the capability  
 434 to assess hydrological responses to climate variability and change. However, cold regions such as the  
 435 Mackenzie River Basin often have sparse surface observations, particularly at high elevations and latitudes  
 436 where a large amount of runoff is generated, or important cyrspheric processes are impacting the

437 hydrology A novel approach to developing a long-term data set using the WFDEI-GEM-CaPA approach  
438 outlined above was necessary to better understand and represent the seasonal/inter-annual variability of  
439 hydrological fluxes and the timing of runoff, and their long-term trends. This dataset is also valuable for  
440 bias correction of climate model projections to assess potential impacts of future climate change on the  
441 hydrology and water resources of the basin.

442 The raw CanRCM4 outputs were found to have systematic biases, which required bias correction  
443 towards WFDEI-GEM-CaPA. There are clear discrepancies between the seasonal cycle of WFDEI-GEM-  
444 CaPA, raw, and bias-corrected CanRCM4 data. For example, the CanRCM4 simulated climatological daily  
445 mean precipitation in June over the MRB between 1979 – 2008 is ~2.5 mm/day while the observed value  
446 is ~1.5 mm/day. This results in a 1.0 mm/day wet bias which can have various implications for quantifying  
447 water resources availability, management and adaptation in a future changed climate. Therefore, it was  
448 crucial to produce the bias-corrected CanRCM4 outputs prior to using the data to drive large scale  
449 hydrological models for climate change impacts analysis in the MRB. Nevertheless, the WFDEI-GEM-CaPA  
450 dataset, used here as the reference, has uncertainties (although it is superior to WFDEI as shown in Figs.  
451 6-11) and should be used with caution especially from the perspective of over-interpreting impact model  
452 outputs.

#### 453 **Data availability**

454 The final product (WFDEI-GEM-CaPA, 1979-2016) is freely available at the Federated Research  
455 Data Repository at <http://dx.doi.org/10.20383/101.0111> (Asong et al., 2018) while the original (raw) and  
456 corrected CanRCM4 data are also freely available at <https://doi.org/10.20383/101.0162> (Asong et al.,  
457 2019).

458 **Author contribution**

459 Z.E., H.W., J.P., A.P., and M.E. conceived and designed the experiment. D.P. preprocessed the  
460 GEM-CaPA data, A.C. developed the bias correction model code and guided the computing procedures  
461 while Z.E. performed the computations. M.E extracted the sample data used in generating Figures 4 and  
462 5. M.E. and Z.E. performed the validation against station observations. Z.E. and M.E. prepared the  
463 manuscript with contributions from all co-authors.

464 **Competing interests**

465 The authors declare that they have no conflict of interest.

466 **Acknowledgements**

467 Financial support from the Canada Excellence Research Chair in Water Security, the NSERC  
468 Changing Cold Regions Network and the Global Water Futures program is gratefully acknowledged.  
469 Thanks are due to the Meteorological Service of Canada for providing access to the GEM-CaPA data used  
470 in this study. We also thank Dr. Graham Weedon for making available the WFDEI dataset. We also  
471 appreciate the efforts of Amber Peterson, Data Manager, Global Institute for Water Security toward  
472 archiving the data at the Federated Research Data Repository.

473

474

475

476

477

478

479 **References**

480 Alavi, N., Bélair, S., Fortin, V., Zhang, S., Husain, S. Z., Carrera, M. L., and Abrahamowicz, M.: Warm  
481 Season Evaluation of Soil Moisture Prediction in the Soil, Vegetation, and Snow (SVS) Scheme, *Journal of*  
482 *Hydrometeorology*, 17, 2315-2332, 2016.

483 Asong, Z. E., Khaliq, M. N., and Wheeler, H. S.: Projected changes in precipitation and temperature  
484 over the Canadian Prairie Provinces using the Generalized Linear Model statistical downscaling approach,  
485 *Journal of Hydrology*, 539, 429-446, 2016b.

486 Asong, Z. E., Razavi, S., Wheeler, H. S., and Wong, J. S.: Evaluation of Integrated Multi-satellitE  
487 Retrievals for GPM (IMERG) over Southern Canada against Ground Precipitation Observations: A  
488 Preliminary Assessment, *Journal of Hydrometeorology*, 0, null, 2017a.

489 Asong, Z. E., Razavi, S., Wheeler, H. S., and Wong, J. S.: Evaluation of Integrated Multisatellite  
490 Retrievals for GPM (IMERG) over Southern Canada against Ground Precipitation Observations: A  
491 Preliminary Assessment, *Journal of Hydrometeorology*, 18, 1033-1050, 2017b.

492 Asong, Z. E., Wheeler, H., Pomeroy, J., Pietroniro, A., and Elshamy, M.: A Bias-Corrected 3-hourly  
493 0.125 Gridded Meteorological Forcing Data Set (1979 – 2016) for Land Surface Modeling in North America.  
494 2018.

495 Asong, Z. E., Wheeler, H., Pomeroy, J., Pietroniro, A., Elshamy, M., Princz, D., and Cannon, A.: High-  
496 Resolution Meteorological Forcing Data for Hydrological Modelling and Climate Change Impact Analysis  
497 in Mackenzie River Basin. 2019.

498 Barnett, T. P., Adam, J. C., and Lettenmaier, D. P.: Potential impacts of a warming climate on water  
499 availability in snow-dominated regions, *Nature*, 438, 303, 2005.

500 Behnke, R., Vavrus, S., Allstadt, A., Albright, T., Thogmartin, W. E., and Radeloff, V. C.: Evaluation  
501 of downscaled, gridded climate data for the conterminous United States, *Ecological Applications*, 26,  
502 1338-1351, 2016.

503 Beniston, M.: Climatic change in mountain regions: a review of possible impacts. In: *Climate*  
504 *variability and change in high elevation regions: Past, present & future*, Springer, 2003.

505 Boluwade, A., Zhao, K. Y., Stadnyk, T. A., and Rasmussen, P.: Towards validation of the Canadian  
506 precipitation analysis (CaPA) for hydrologic modeling applications in the Canadian Prairies, *Journal of*  
507 *Hydrology*, 556, 1244-1255, 2018.

508 Brody, S. D., Zahran, S., Maghelal, P., Grover, H., and Highfield, W. E.: The Rising Costs of Floods:  
509 Examining the Impact of Planning and Development Decisions on Property Damage in Florida, *Journal of*  
510 *the American Planning Association*, 73, 330-345, 2007.

511 Cannon, A. J.: Multivariate quantile mapping bias correction: an N-dimensional probability density  
512 function transform for climate model simulations of multiple variables, *Climate Dynamics*, 50, 31-49,  
513 2018.

514 Cannon, A. J., Sobie, S. R., and Murdock, T. Q.: Bias Correction of GCM Precipitation by Quantile  
515 Mapping: How Well Do Methods Preserve Changes in Quantiles and Extremes?, *Journal of Climate*, 28,  
516 6938-6959, 2015.

517 Chadburn, S. E., Burke, E. J., Essery, R. L. H., Boike, J., Langer, M., Heikenfeld, M., Cox, P. M., and  
518 Friedlingstein, P.: Impact of model developments on present and future simulations of permafrost in a  
519 global land-surface model, *The Cryosphere*, 9, 1505-1521, 2015.

520 Chen, J., Brissette, F. P., Chaumont, D., and Braun, M.: Finding appropriate bias correction  
521 methods in downscaling precipitation for hydrologic impact studies over North America, *Water Resources*  
522 *Research*, 49, 4187-4205, 2013.

523 Chen, J., Li, C., Brissette, F. P., Chen, H., Wang, M., and Essou, G. R. C.: Impacts of correcting the  
524 inter-variable correlation of climate model outputs on hydrological modeling, *Journal of Hydrology*, 560,  
525 326-341, 2018.

526 Coopersmith, E. J., Minsker, B. S., and Sivapalan, M.: Patterns of regional hydroclimatic shifts: An  
527 analysis of changing hydrologic regimes, *Water Resources Research*, 50, 1960-1983, 2014.

528 DeBeer, C. M., Wheeler, H. S., Carey, S. K., and Chun, K. P.: Recent climatic, cryospheric, and  
529 hydrological changes over the interior of western Canada: a review and synthesis, *Hydrol. Earth Syst. Sci.*,  
530 20, 1573-1598, 2016.

531 Demaria, E. M. C., Roundy, J. K., Wi, S., and Palmer, R. N.: The Effects of Climate Change on  
532 Seasonal Snowpack and the Hydrology of the Northeastern and Upper Midwest United States, *Journal of*  
533 *Climate*, 29, 6527-6541, 2016.

534 Dibike, Y., Prowse, T., Bonsal, B., and O'Neil, H.: Implications of future climate on water availability  
535 in the western Canadian river basins, *International Journal of Climatology*, doi: 10.1002/joc.4912, 2016.  
536 n/a-n/a, 2016.

537 Diffenbaugh, N. S., Scherer, M., and Ashfaq, M.: Response of snow-dependent hydrologic  
538 extremes to continued global warming, *Nature Climate Change*, 3, 379, 2012.

539 Dumanski, S., Pomeroy, J. W., and Westbrook, C. J.: Hydrological regime changes in a Canadian  
540 Prairie basin, *Hydrological Processes*, 29, 3893-3904, 2015.

541 Eum, H.-I., Dibike, Y., Prowse, T., and Bonsal, B.: Inter-comparison of high-resolution gridded  
542 climate data sets and their implication on hydrological model simulation over the Athabasca Watershed,  
543 Canada, *Hydrological Processes*, 28, 4250-4271, 2014.

544 Fang, X., Pomeroy, J. W., Ellis, C. R., MacDonald, M. K., DeBeer, C. M., and Brown, T.: Multi-variable  
545 evaluation of hydrological model predictions for a headwater basin in the Canadian Rocky Mountains,  
546 *Hydrol. Earth Syst. Sci.*, 17, 1635-1659, 2013.

547 Fortin, V., Jean, M., Brown, R., and Payette, S.: Predicting snow depth in a forest–tundra landscape  
548 using a conceptual model allowing for snow redistribution and constrained by observations from a digital  
549 camera, *Atmosphere-Ocean*, 53, 200-211, 2015a.

550 Fortin, V., Roy, G., Donaldson, N., and Mahidjiba, A.: Assimilation of radar quantitative  
551 precipitation estimations in the Canadian Precipitation Analysis (CaPA), *Journal of Hydrology*, 531, Part 2,  
552 296-307, 2015b.

553 Gbambie, A. S. B., Poulin, A., Boucher, M.-A., and Arsenault, R.: Added Value of Alternative  
554 Information in Interpolated Precipitation Datasets for Hydrology, *Journal of Hydrometeorology*, 18, 247-  
555 264, 2017.

556 Gudmundsson, L., Bremnes, J. B., Haugen, J. E., and Engen-Skaugen, T.: Technical Note:  
557 Downscaling RCM precipitation to the station scale using statistical transformations &ndash; a  
558 comparison of methods, *Hydrol. Earth Syst. Sci.*, 16, 3383-3390, 2012.

559 Hou, A. Y., Kakar, R. A., Neeck, S., Azarbarzin, A. A., Kummerow, C. D., Kojima, M., Oki, R.,  
560 Nakamura, K., and Iguchi, T.: The Global Precipitation Measurement Mission, *Bulletin of the American*  
561 *Meteorological Society*, 95, 701-722, 2014.

562 IPCC: Climate Change 2013: The Physical Science Basis. Contribution of Working Group I to the  
563 Fifth Assessment Report of the Intergovernmental Panel on Climate Change, Cambridge University Press,  
564 Cambridge, United Kingdom and New York, NY, USA, 2013.

565 Islam, S. u., Déry, S. J., and Werner, A. T.: Future Climate Change Impacts on Snow and Water  
566 Resources of the Fraser River Basin, British Columbia, *Journal of Hydrometeorology*, 18, 473-496, 2017.

567 Kane, D. L., Hinzman, L. D., Woo, M.-k., and Everett, K. R.: Arctic hydrology and climate change.  
568 In: *Arctic ecosystems in a changing climate*, Elsevier, 1991.

569 Mahfouf, J. F., Brasnett, B., and Gagnon, S.: A Canadian precipitation analysis (CaPA) project:  
570 Description and preliminary results, *Atmosphere-Ocean*, 45, 1-17, 2007.

571 Maraun, D.: Bias Correcting Climate Change Simulations - a Critical Review, *Current Climate*  
572 *Change Reports*, 2, 211-220, 2016.



573 Maraun, D.: Bias Correction, Quantile Mapping, and Downscaling: Revisiting the Inflation Issue,  
574 *Journal of Climate*, 26, 2137-2143, 2013.

575 Maraun, D., Shepherd, T. G., Widmann, M., Zappa, G., Walton, D., Gutiérrez, J. M., Hagemann, S.,  
576 Richter, I., Soares, P. M. M., Hall, A., and Mearns, L. O.: Towards process-informed bias correction of  
577 climate change simulations, *Nature Climate Change*, 7, 764, 2017.

578 Maraun, D., Wetterhall, F., Ireson, A. M., Chandler, R. E., Kendon, E. J., Widmann, M., Brienen, S.,  
579 Rust, H. W., Sauter, T., Themeßl, M., Venema, V. K. C., Chun, K. P., Goodess, C. M., Jones, R. G., Onof, C.,  
580 Vrac, M., and Thiele-Eich, I.: Precipitation downscaling under climate change: Recent developments to  
581 bridge the gap between dynamical models and the end user, *Reviews of Geophysics*, 48, 2010.

582 Martin, E. and Etchevers, P.: Impact of Climatic Changes on Snow Cover and Snow Hydrology in  
583 the French Alps. In: *Global Change and Mountain Regions: An Overview of Current Knowledge*, Huber, U.  
584 M., Bugmann, H. K. M., and Reasoner, M. A. (Eds.), Springer Netherlands, Dordrecht, 2005.

585 Meyer, J., Kohn, I., Stahl, K., Hakala, K., Seibert, J., and Cannon, A. J.: Effects of univariate and  
586 multivariate bias correction on hydrological impact projections in alpine catchments, *Hydrol. Earth Syst.*  
587 *Sci.*, 23, 1339-1354, 2019.

588 Milly, P. C. D., Betancourt, J., Falkenmark, M., Hirsch, R. M., Kundzewicz, Z. W., Lettenmaier, D. P.,  
589 and Stouffer, R. J.: Stationarity Is Dead: Whither Water Management?, *Science*, 319, 573-574, 2008.

590 Park, H., Yoshikawa, Y., Oshima, K., Kim, Y., Ngo-Duc, T., Kimball, J. S., and Yang, D.: Quantification  
591 of Warming Climate-Induced Changes in Terrestrial Arctic River Ice Thickness and Phenology, *Journal of*  
592 *Climate*, 29, 1733-1754, 2016.

593 Pomeroy, J. W. and Li, L.: Prairie and arctic areal snow cover mass balance using a blowing snow  
594 model, *Journal of Geophysical Research: Atmospheres*, 105, 26619-26634, 2000.

595 Prowse, T. D. and Beltaos, S.: Climatic control of river-ice hydrology: a review, *Hydrological*  
596 *processes*, 16, 805-822, 2002.

597 Reiter, P., Gutjahr, O., Schefczyk, L., Heinemann, G., and Casper, M.: Bias correction of ENSEMBLES  
598 precipitation data with focus on the effect of the length of the calibration period, *Meteorologische*  
599 *Zeitschrift*, 25, 85-96, 2016.

600 Sapiano, M. R. P. and Arkin, P. A.: An Intercomparison and Validation of High-Resolution Satellite  
601 Precipitation Estimates with 3-Hourly Gauge Data, *Journal of Hydrometeorology*, 10, 149-166, 2009.

602 Schoetter, R., Hoffmann, P., Rechid, D., and Schlünzen, K. H.: Evaluation and Bias Correction of  
603 Regional Climate Model Results Using Model Evaluation Measures, *Journal of Applied Meteorology and*  
604 *Climatology*, 51, 1670-1684, 2012.

605 Schulzweida, U., Kornblueh, L., and Quast, R.: Climate data operators, Max-Planck-Institute for  
606 Meteorology, Hamburg and <http://www.mpimet.mpg.de/~cdo>, 2004. 2004.

607 Sheffield, J., Goteti, G., and Wood, E. F.: Development of a 50-Year High-Resolution Global Dataset  
608 of Meteorological Forcings for Land Surface Modeling, *Journal of Climate*, 19, 3088-3111, 2006.

609 Sippel, S., Otto, F. E. L., Forkel, M., Allen, M. R., Guillod, B. P., Heimann, M., Reichstein, M.,  
610 Seneviratne, S. I., Thonicke, K., and Mahecha, M. D.: A novel bias correction methodology for climate  
611 impact simulations, *Earth Syst. Dynam.*, 7, 71-88, 2016.

612 Stocker, T. F., Qin, D., Plattner, G.-K., Alexander, L. V., Allen, S. K., Bindoff, N. L., Bréon, F.-M.,  
613 Church, J. A., Cubasch, U., Emori, S., Forster, P., Friedlingstein, P., Gillett, N., Gregory, J. M., Hartmann, D.  
614 L., Jansen, E., Kirtman, B., Knutti, R., Krishna Kumar, K., Lemke, P., Marotzke, J., Masson-Delmotte, V.,  
615 Meehl, G. A., Mokhov, I. I., Piao, S., Ramaswamy, V., Randall, D., Rhein, M., Rojas, M., Sabine, C., Shindell,  
616 D., Talley, L. D., Vaughan, D. G., and Xie, S.-P.: Technical Summary. In: *Climate Change 2013: The Physical  
617 Science Basis. Contribution of Working Group I to the Fifth Assessment Report of the Intergovernmental  
618 Panel on Climate Change*, Stocker, T. F., Qin, D., Plattner, G.-K., Tignor, M., Allen, S. K., Boschung, J., Nauels,  
619 A., Xia, Y., Bex, V., and Midgley, P. M. (Eds.), Cambridge University Press, Cambridge, United Kingdom and  
620 New York, NY, USA, 2013.

621 Storch, H. v.: On the Use of “Inflation” in Statistical Downscaling, *Journal of Climate*, 12, 3505-  
622 3506, 1999.

623 Taylor, K. E., Stouffer, R. J., and Meehl, G. A.: An Overview of CMIP5 and the Experiment Design,  
624 *Bulletin of the American Meteorological Society*, 93, 485-498, 2012.

625 Vincent, L. A., Zhang, X., Brown, R. D., Feng, Y., Mekis, E., Milewska, E. J., Wan, H., and Wang, X.  
626 L.: Observed Trends in Canada’s Climate and Influence of Low-Frequency Variability Modes, *Journal of  
627 Climate*, 28, 4545-4560, 2015.

628 Wang, X. L. and Lin, A.: An algorithm for integrating satellite precipitation estimates with in situ  
629 precipitation data on a pentad time scale, *Journal of Geophysical Research: Atmospheres*, 120, 3728-3744,  
630 2015.

631 Weedon, G. P., Balsamo, G., Bellouin, N., Gomes, S., Best, M. J., and Viterbo, P.: The WFDEI  
632 meteorological forcing data set: WATCH Forcing Data methodology applied to ERA-Interim reanalysis  
633 data, *Water Resources Research*, 50, 7505-7514, 2014.

634 Wong, J. S., Razavi, S., Bonsal, B. R., Wheeler, H. S., and Asong, Z. E.: Inter-comparison of daily  
635 precipitation products for large-scale hydro-climatic applications over Canada, *Hydrol. Earth Syst. Sci.*, 21,  
636 2163-2185, 2017.

637           Woo, M.-K. and Pomeroy, J.: Snow and Runoff: Processes, Sensitivity and Vulnerability. In:  
638 Changing Cold Environments, John Wiley & Sons, Ltd, 2011.

639           Yeh, K.-S., Côté, J., Gravel, S., Méthot, A., Patoine, A., Roch, M., and Staniforth, A.: The CMC–MRB  
640 Global Environmental Multiscale (GEM) Model. Part III: Nonhydrostatic Formulation, Monthly Weather  
641 Review, 130, 339-356, 2002.

642